Available online at www.sciencedirect.com

SCIENCE DIRECT

Developmental Biology 292 (2006) 174–188

DEVELOPMENTAL BIOLOGY

www.elsevier.com/locate/ydbio

Zebrafish *foxd3* is selectively required for neural crest specification, migration and survival

Rodney A. Stewart [a], Brigitte L. Arduini [b], Stephane Berghmans [a], Rani E. George [a], John P. Kanki [a,*], Paul D. Henion [b,*], A. Thomas Look [a,*]

[a] *Department of Pediatric Oncology, Dana-Farber Cancer Institute, 44 Binney Street, Boston, MA 02115, USA*

[b] *Center for Molecular Neurobiology, Department of Neuroscience, Department of Molecular Genetics, Ohio State University, Columbus, OH 43210, USA*

Received for publication 1 July 2005; revised 23 November 2005; accepted 19 December 2005

Abstract

The vertebrate neural crest is a pluripotent cell population that generates a large variety of cell types, including peripheral neurons, cartilage and pigment cells. Mechanisms that control the patterning of the neural crest toward specific cell fates remain only partially understood. Zebrafish homozygous for the *sympathetic mutation 1* (*sym1*) have defects in a subset of neural crest derivatives, such as peripheral neurons, glia and cartilage, but retain normal numbers of melanocytes. The *sym1* mutation is a nucleotide deletion that disrupts the forkhead DNA-binding domain of the *foxd3* gene, which encodes a conserved winged-helix transcription factor. We show that *sym1* mutants have normal numbers of premigratory neural crest cells, but these cells express reduced levels of *snai1b* and *sox10*, implicating *foxd3* as an essential regulator of these transcription factors in the premigratory neural crest. The onset of neural crest migration is also delayed in *sym1* mutants, and there is a reduction in the number of migratory trunk neural crest cells, particularly along the medial migration pathway. TUNEL analysis revealed aberrant apoptosis localized to the hindbrain neural crest at the 15-somite stage, indicating a critical role for *foxd3* in the survival of a subpopulation of neural crest cells. These results show that *foxd3* selectively specifies premigratory neural crest cells for a neuronal, glial or cartilage fate, by inducing the expression of lineage-associated transcription factors in these cells and regulating their subsequent migration.

Keywords: Neural crest; *foxd3*; Sympathetic; *sox10*; *snai1b*; Survival; Migration; Specification; Zebrafish

Introduction

The vertebrate neural crest is a transient population of embryonic precursor cells that gives rise to a variety of cell types, including neurons and glia of the peripheral nervous system, chromatophores, and elements of the craniofacial skeleton (LeDouarin and Kalcheim, 1999; Moury and Jacobson, 1989). As the neural crest develops in the dorsal neural tube, progenitor cells located at the neural plate border undergo an epithelial–mesenchymal transition leading to formation of the premigratory neural crest. These cells subsequently migrate along stereotyped pathways to specific locations throughout the embryo, where they differentiate and generate diverse tissues. While some of the regulatory mechanisms controlling the latter stages of neural crest differentiation have been identified (LeDouarin and Kalcheim, 1999), the genetic pathways mediating the induction of neural crest and the early specification of different neural crest cell sublineages remain unclear. Evidence suggests that the fates of many neural crest cells can be determined very early in development (Henion and Weston, 1997; Luo et al., 2003a,b; Raible and Eisen, 1994; Reedy et al., 1998; Schilling and Kimmel, 1994; Wilson et al., 2004), raising the possibility that genes involved in the induction and generation of neural crest may also be required for neural crest development in a lineage-restricted fashion.

During gastrulation, cells at the border between neural and non-neural ectoderm are induced to give rise to neural crest cells through the cumulative effects of Wnt, Bmp and Fgf signals

* Corresponding authors.
E-mail addresses: john_kanki@dfci.harvard.edu (J.P. Kanki), henion.1@osu.edu (P.D. Henion), thomas_look@dfci.harvard.edu (A.T. Look).

0012-1606/$ - see front matter © 2006 Elsevier Inc. All rights reserved.
doi:10.1016/j.ydbio.2005.12.035

originating from adjacent ectodermal and mesodermal tissues (Huang and Saint-Jeannet, 2004; Knecht and Bronner-Fraser, 2002). Neural plate border and/or neural crest cells co-express numerous transcription factors, including *foxd3*, *snail/slug*, *sox10* and *tfap2a,* that have critical roles in neural crest development (Gammill and Bronner-Fraser, 2003), but how these genes direct the subsequent specification of neural crest sublineages remains unclear.

Foxd3 has been proposed to play an important role in the early stages of neural crest development because it is widely expressed by neural crest progenitors at the neural plate border in all vertebrate species studied to date (Dottori et al., 2001; Kos et al., 2001; Pohl and Knochel, 2001; Sasai et al., 2001). *foxd3* expression is maintained in the premigratory neural crest cells but is rapidly downregulated as neural crest cells differentiate and migrate. Functional studies in frogs and chicks, using forced expression of wild-type, dominant-negative or antisense forms of *foxd3*, have shown that Foxd3 regulates the expression of early neural crest genes in the developing neural tube, suggesting an instructive role during neural crest induction. However, these findings have been inconsistent, because both loss-of-function and gain-of-function experiments showed an increase in the early expression of neural crest genes, likely reflecting a *foxd3* negative-autoregulatory mechanism (Dottori et al., 2001; Kos et al., 2001; Pohl and Knochel, 2001; Sasai et al., 2001). More recent studies using in ovo electroporation to force *foxd3* expression into the chick neural tube, suggest *foxd3* may play a more important role during neural crest migration, by regulating the expression of cell–cell adhesion molecules (Cheung et al., 2005). Together, these studies indicate the importance of Foxd3 during neural crest development, but the lack of an in vivo mutant model has made it difficult to determine at what stage this transcription factor is necessary for neural crest development, and whether it is required for the development and migration of all neural crest cells or only specific sublineages. Attempts to elucidate the function of Foxd3 through murine gene-knockout strategies have been hampered by embryonic lethality, which prevents full analysis of the developing neural crest (Hanna et al., 2002).

Zebrafish *foxd3* is expressed during gastrulation by cells of the neural plate border, in posterior and ventral tailbud mesoderm and transiently in the developing floor plate (Odenthal and Nusslein-Volhard, 1998). Expression of this gene is then observed in premigratory neural crest cells of the head and trunk but is generally extinguished prior to the onset of migration, except for a subset of migrating cranial neural crest cells that transiently express *foxd3*. As *foxd3* expression becomes downregulated in trunk neural crest cells, expression is initiated in the somites and also later in some developing peripheral glia (Gilmour et al., 2002; Kelsh et al., 2000).

Using an ENU-induced mutagenesis screen to identify genes required for normal development of the zebrafish peripheral sympathetic nervous system, we recovered an embryonic lethal mutant, *sympathetic mutation 1* (*sym1*) that lacks sympathetic neurons and displays craniofacial defects. We have determined that the molecular lesion at the *sym1* locus results in a functional null allele of the zebrafish *foxd3* gene. Unlike *foxd3* mutant mice, homozygous *sym1* mutant embryos survive throughout all stages of embryonic neural crest development, allowing *foxd3* function to be critically accessed during the generation of the neural crest and its derivatives.

Materials and methods

Animal husbandry and cell counts

Zebrafish were maintained, mutagenized and bred as described (Westerfield, 1993). *sym1* mutants were initially identified by phenotype and *th* expression, with subsequent confirmation by genotyping. Cell counts for differentiated pigment cells were performed in live embryos in three separate regions, (the dorsal, lateral and ventral stripes), at 3, 4 and 5 days post-fertilization (dpf). We counted migrating trunk neural crest cells after in situ hybridization (ISH) for *sox10*, *ctn*, *dct* and *mitf* in the 3–15 somite region at 24, 36 and 48 h post-fertilization (hpf). Premigratory cell counts were performed at the level of somites 3–5 (inclusive) in pairs of 12 somite-stage embryos. The average counts agreed with those of neural crest cells identified morphologically (Raible et al., 1992) and molecularly (Luo et al., 2001) in wild-type embryos.

Molecular biology and cloning

The F1 WIK female harboring the *sym1* mutation was outcrossed to the AB strain for genetic mapping and to generate F2 and F3 generations. Genomic DNAs from 40 wild-type and mutant embryos were pooled and screened for linkage to a set of 239 CA markers; this analysis places the *sym1* mutation on chromosome 6. Further genetic linkage analysis using additional markers on chromosome 6 placed marker z10183 less than 1 cM from the *sym1* mutation. The *foxd3* full-length clone used for RNA synthesis and in situ hybridization experiments is described elsewhere (Kelsh et al., 2000; Odenthal and Nusslein-Volhard, 1998). The sequence harboring the *foxd3* exon was obtained from the Sanger genomic trace sequence repository and analyzed with SeqMan alignment software (DNASTAR, Inc.). Genotyping was performed by extracting genomic DNA from embryos after ISH as described (Westerfield, 1993), and sequencing the *foxd3* gene directly, or using a pair of allele-specific PCR primers that only amplify the wild-type or *sym1* allele respectively. The primers for PCR genotyping are: Wild-type, forward 5′CCCAGTCGGAAGATATG3′, Reverse, 5′CGGACGAATTGTCCAGTG-3′. *sym1* Forward, 5′GAAGAAGTTGACGC-TCAGTGGAATC-3′, Reverse, 5′-TTTCGACAACGGTAGCTTTCT GAG-3′.

Whole-mount in situ hybridization, immunostaining and microinjections

Full-length, capped-sense and antisense *foxd3* RNAs were generated with Message Machine, and a Poly-A tail was added with a Poly(A) tailing kit (Ambion). Based on the published GenBank sequence (NM_131290) for *foxd3,* a morpholino (MO) was designed: CACCGCGCACTTTGCTGCTGGAGCA (Gene Tools, Inc.). Whole-mount in situ hybridization was carried out as described by (Thisse et al., 1993). Antisense probes were generated as described for c-*ret* (Bisgrove et al., 1997), *dlx2* (Akimenko et al., 1994), *ctn* (Luo et al., 2001), *foxd3*/*fkd6* (Kelsh et al., 2000), *zash1a* (Allende and Weinberg, 1994), *mitf* and *dct*, (Lister et al., 1999), *xdh* (Parichy et al., 2000b), *ednrb1* (Parichy et al., 2000a), *tfap2a* (Knight et al., 2003), *snai1b* (Thisse et al., 1995), *sox10* (Dutton et al., 2001), *myoD* (Weinberg et al., 1996), *twhh* (Ekker et al., 1995), *col2a1* (Yan et al., 1995) and *sox9a* (Chiang et al., 2001). The *phox2b* probe, a generous gift of Dr. Su Guo, was generated by digestion with *Eco*R*1* followed by transcription with T3 RNA polymerase. Cartilage staining with Alcian blue was performed as previously described (Kimmel et al., 1998). Whole-mount antibody staining with anti-Hu mAb 16A11 (Molecular Probes) was performed on embryos fixed for 2 h at RT in 4% PFA, as described by (An et al., 2002). Frozen sections of embryos processed for in situ hybridization were generated as described by Luo et al., (2001).

TUNEL assays

Apoptosis was detected in embryos by terminal transferase dUTP nick-end labeling (TUNEL), according to the manufacturer's protocols (In Situ Cell Death Detection Kit: POD and AP; Roche). After labeling, the embryos were washed with PBS (3×) and blocked in 4% goat serum for 30 min; antifluorescein antibody (1:5000) was added and incubated at 4°C overnight. The embryos were washed in PBS (3×) and stained with VECTORSTAIN® Elite ABC kits (Vector (r) labs) to detect AP or POD activity, according to the manufacturers protocol.

Results

Defects in peripheral neuron and glial derivatives in sym1 mutants

To identify genes regulating peripheral sympathetic nervous system development, we performed a forward genetic screen for mutations that disrupt the development of sympathetic neurons in embryos at 5 dpf. Developing zebrafish sympathetic ganglia were readily identified at 2 dpf, using whole-mount ISH to detect expression of *tyrosine hydroxylase* (*th*) mRNA, which is required for catecholamine biosynthesis in noradrenergic and dopaminergic neurons (Figs. 1A, B; An et al., 2002; Stewart et al., 2004). The first mutant recovered from this screen was *sym1* (*sympathetic mutation 1*), which showed a dramatic reduction or complete loss of *th* expression in developing sympathetic neurons (Figs. 1E, F). The mutation specifically affected neural crest-derived noradrenergic neurons because *th* expression in dopaminergic neurons of the CNS was not affected (Fig. 1E). Analysis of the superior sympathetic cervical ganglion in *sym1* mutants between 2 and 3 dpf indicated that *th* was not expressed in this region (Fig. 1F), nor were Hu-positive neurons found in the cervical ganglion of mutant embryos (data not shown).

To determine whether sympathoadrenal progenitor cells are present in *sym1* mutants, we examined the expression of *zash1a*,

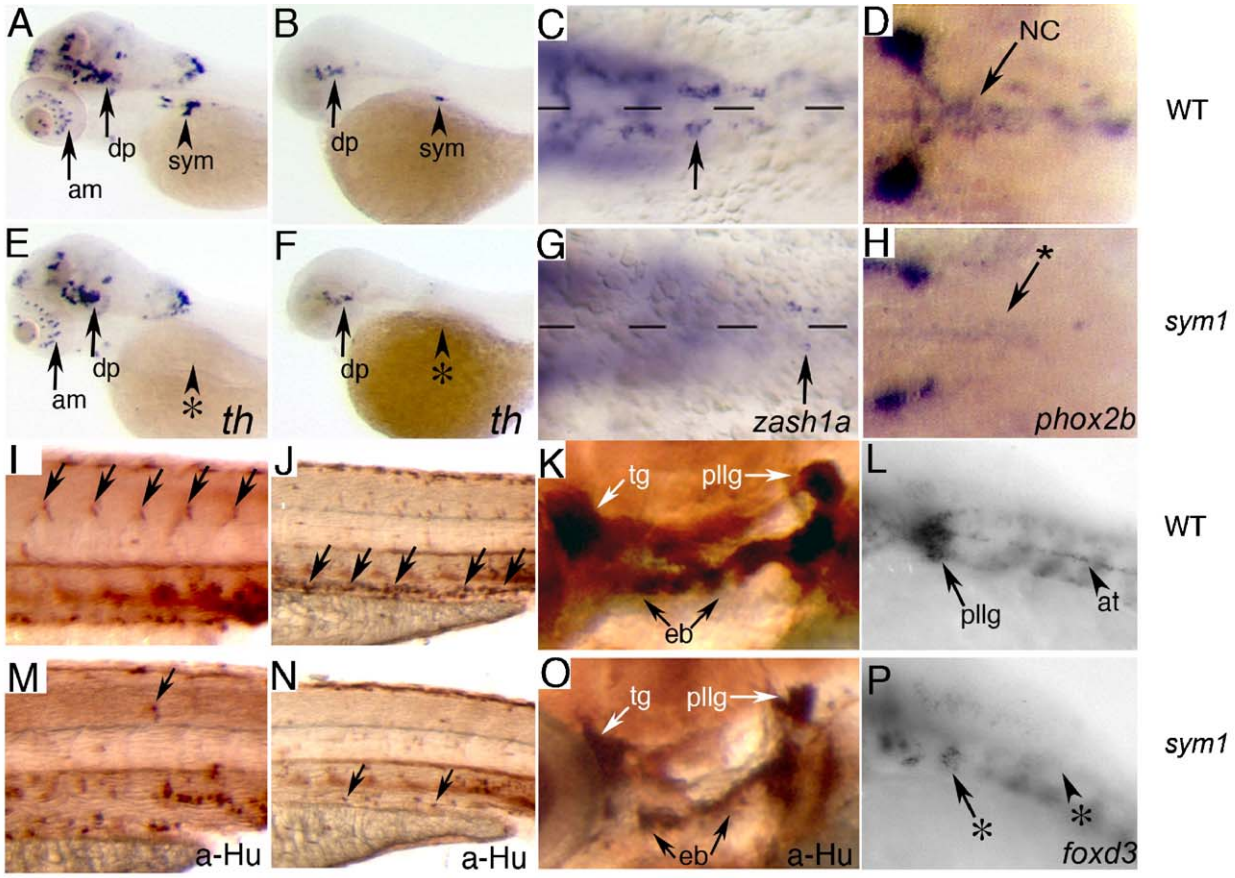

Fig. 1. *sym1* mutants have defects in trunk and vagal neural crest-derived peripheral neurons, cranial ganglion neurons and glia. Lateral views of wild-type (A, B) and *sym1* mutant (E, F) embryos showing tyrosine hydroxylase (*th*) expression at 5 dpf (A, E) and 48 hpf (B, F). There is a dramatic reduction in the number of *th*-positive cells in the region of the developing sympathetic cervical complex (arrowheads) in *sym1* mutants (0–2 cells at 2 dpf, 0–10 cells at 5 dpf, $n = 10$), compared to their wild-type siblings (10–15 cells at 2 dpf, 40–50 cells at 5 dpf, $n = 10$). High magnification ventral views of wild-type (C, D) and *sym1* mutant (G, H) embryos, showing that the loss of sympathetic neurons in *sym1* mutants is reflected by a severely reduced number of sympathoblasts based on *zash1a* expression at 40 hpf (C, G) and *phox2b* expression at 48 hpf (D, H). Arrows in C, D, G, H indicate migrating sympathoblasts. Lateral views of wild-type (I–L) and *sym1* mutant (M–P) embryos. Black arrows indicate position of developing DRG (I) and enteric neurons (J) in 3 dpf wild-type embryos, which are largely absent in *sym1* mutants (M, N). The cranial ganglion neurons at 3 dpf are reduced in size in *sym1* mutants by approximately 30% (K compared to O). White arrows indicate the trigeminal (tg) and posterior lateral line (pllg) ganglia complex. Black arrows indicate epibranchial ganglia (eb). (L, P) *foxd3* is expressed in developing glia associated with the posterior lateral line ganglia (arrow) and axon tract (arrowhead) in wild-type embryos at 48 hpf (L), but is severely reduced or absent in *sym1* mutant embryos (P). Abbreviations: absence of expressing cells (*), amacrine cells (am), axon tract (at), dopaminergic neurons (dp), hindbrain (hb), neural crest-derived enteric and sympathetic precursors (NC), sympathetic neurons (sym).

the earliest marker of sympathetic neuron differentiation (Figs. 1C, G; (Stewart et al., 2004). At 40 hpf, more than 20 *zash1a*$^+$ cells (sympathoblasts) were consistently detected in wild-type embryos, and they migrated ventrally to the dorsal aorta (Fig. 1C). *zash1a* expression was not evident adjacent to the dorsal aorta in *sym1* mutant embryos, although one or two dorsally displaced *zash1a*$^+$ cells were occasionally observed (Fig. 1G). The neurogenic marker *phox2b* is expressed downstream of *zash1a* during development of the sympathetic nervous system (Stewart et al., 2004). In zebrafish, *phox2b* is normally expressed in neural crest-derived cells that are concentrated adjacent to the dorsal aorta and in the region of the anterior gut tube at the ventral midline, and subsequently differentiate into sympathetic or enteric precursors (Shepherd et al., 2004). Consistent with the loss of *zash1a* expression in migrating sympathoblasts, *phox2b*-expressing sympathetic or enteric precursors were not observed in mutant embryos (Fig. 1H). These results show that the absence of *th* expression in the developing sympathetic ganglia is due to loss of sympathetic progenitors, rather than failure of these cells to differentiate into peripheral sympathetic nervous system neurons.

We next examined the development of dorsal root (DRG), enteric and cranial ganglion neurons in *sym1* embryos. In wild-type embryos, trunk neural crest-derived DRG sensory neurons form bilateral ganglia lateral to the ventral neural tube in each somitic segment. The pan-neural marker Hu-C is expressed in both differentiated and some precursor DRG cells (An et al., 2002). Analysis of anti-Hu positive cells in *sym1* mutants revealed that DRG neurons were completely absent in most *sym1* mutants, although a few mutants had a small, variable number of DRG neurons that appeared both unilaterally and dorsally displaced (Fig. 1M). Loss of the DRG precursor population in *sym1* mutants was confirmed by analysis of the DRG precursor marker *ngn-1* (Ungos et al., 2003), which showed a severe reduction in expression pattern in the region of developing DRG neurons (data not shown). Zebrafish enteric neurons, derived from vagal neural crest cells, initially differentiate in the anterior gut tube and subsequently populate the anterior–posterior extent of the gut. In *sym1* mutant embryos, only a small minority of enteric neurons develop (Figs. 1J, N). The lack of enteric neurons in *sym1* mutants is predicted by the near absence of enteric neuron precursors defined by the expression of *c-ret* and *phox2b* (Fig. 1H; and data not shown; Bisgrove et al., 1997; Marcos-Gutierrez et al., 1997).

In zebrafish, neurons and glia of the cranial ganglia arise from cells of both cranial neural crest and placodal origins, although the relative contribution of each cell type to cranial ganglia development is unknown (Schilling and Kimmel, 1994). Using the pan-neuronal marker Hu-C, we found that the size of all cranial ganglia was reduced by approximately 30% in *sym1* mutants and these smaller structures were often malformed (e.g., the epibranchial ganglia were fused together, Fig. 1O). We also analyzed the development of neural crest-derived peripheral glia in the cranial ganglia of *sym1* mutant embryos, using the *foxd3* and *sox10* markers, which are expressed by at least some peripheral glia during development (Gilmour et al., 2002; Kelsh et al., 2000). At 48 hpf, the expression of these markers indicated a reduction of peripheral glia within the cranial ganglia as well as those associated with axons of the lateral line system (Figs. 1L, P; and data not shown).

The development of neural crest-derived chromatophores is delayed in sym1 mutants

Overall, the development of chromatophore sublineages was less affected in *sym1* mutants. The number and morphology of differentiated (melanized) melanophores, for example, were the same in mutant embryos and their wild-type siblings from 3 dpf onwards (Figs. 2A–D, K). However, the differentiation of melanophores was delayed by 3–4 h in mutants compared with their wild-type siblings, and there was a defect in melanophore patterning, with *sym1* mutants containing more dorsally localized cells at 5 dpf (Fig. 2L). Xanthophore development was also delayed in *sym1* mutants, but by 5 dpf it resembled the pattern seen in wild-type siblings (data not shown). The development of silver iridiphores appeared to be significantly affected in *sym1* mutants at 3 dpf, particularly along the trunk (Figs. 2B, D, right arrow), where the mutants contained an average of 7.5 cells compared with 17.5 cells in wild-type siblings ($n = 10$, $P < 0.001$). In contrast, the numbers of iridiphores in the eyes of *sym1* mutants and their wild-type siblings were similar at this stage (Figs. 2B, D, left arrow). By 5 dpf, *sym1* and wild-type embryos had comparable numbers of all chromatophore cell types, although in some individual embryos there was still a decrease (10–20%) in the iridiphore trunk population.

The delayed development of the different chromatophore sublineages was reflected by a delay in the expression of markers that label their respective precursors. For example, the onset of expression of the *microphthalmia-associated transcription factor* (*mitf*) gene by melanophore precursors was delayed in *sym1* mutants by 1–2 h, and revealed defects in trunk neural crest migration (Figs. 2E–H). At 24 hpf, the anterior/posterior extent of *mitf* expression in premigratory neural crest cells in the trunk of *sym1* mutants was almost the same as in their wild-type siblings (Figs. 2E–H arrowheads). However, the ventral migration of *mitf*-positive cells was delayed in *sym1* mutants, because migrating cells were detected at the level of somite-6 in *sym1* mutants, instead of somite-15, where migration had begun in wild-type siblings (Figs. 2E–H, arrows). Similar results were obtained with other chromatophore sublineage markers, including *dct* (*dopachrome tautomerase*, melanophore precursors), *ednrb1* (*endothelin receptor b1*, iridiphore precursors) and *xdh* (*xanthine dehydrogenase*, xanthophore precursors). Normally, these genes are expressed by 19–20 hpf in their respective precursor populations, but in *sym1* mutants they were not expressed until 24 hpf and revealed cell migration defects similar to those noted from analysis of *mitf* expression (data not shown). However, consistent with recovery of the differentiated pigment cell types, the numbers of precursors expressing these genes in *sym1* mutants reached wild-type levels by 36 hpf, as illustrated in Figs. 2I, J for *dct*-expressing cells. Together, these results indicate that in *sym1*

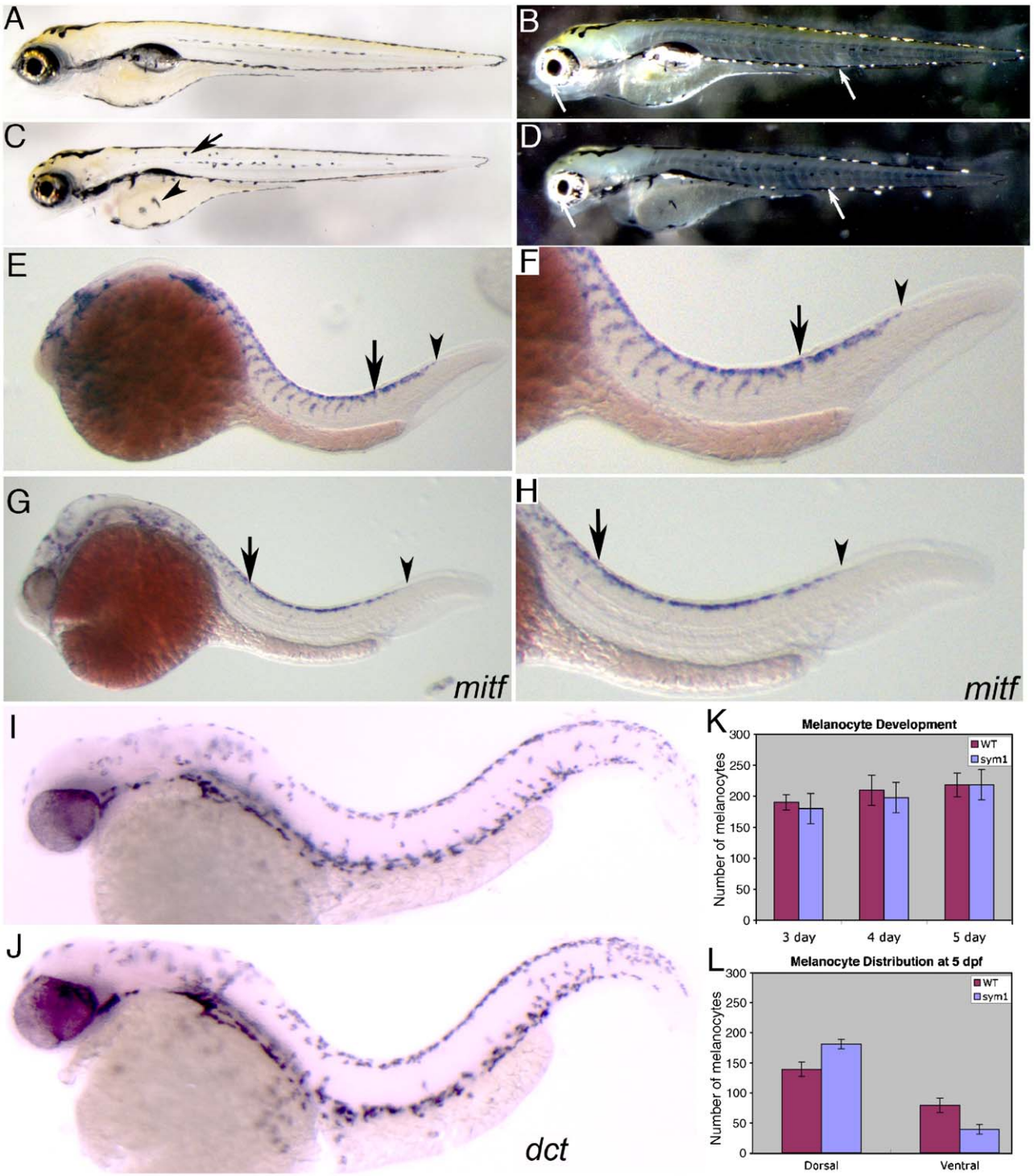

Fig. 2. Development of neural crest-derived chromatophores in *sym1* mutants. Lateral views of living wild-type (A, B) and *sym1* mutant (C, D) embryos at 3 dpf. Melanophores (black) are evident in both wild-type (A) and *sym1* (C) mutant embryos, although *sym1* mutants have more dorsally-displaced melanocytes on the trunk (arrow) and yolk (arrowhead; see also panel L). Incident light reveals silver iridiphores are reduced in some *sym1* mutants (D). Lateral views of developing melanoblasts expressing *mitf* in wild-type (E, F) and *sym1* mutant (G, H) embryos. F and H are higher magnification views of the trunk region in E and G. Arrowheads in E–H indicate the posterior extent of *mitf* staining along the trunk in wild-type and *sym1* mutants, while the arrows in E–H show the posterior extent of dorsal–ventral neural crest migration, both of which are delayed in *sym1* mutants (compare E, F with G, H). Expression of *dct* at 36 hpf in wild-type (I) and *sym1* mutant (J) embryos. The expression pattern and numbers of *dct*-positive cells are indistinguishable between wild-type and *sym1* mutants. Quantitation of melanophore numbers (K) and distribution (L) in wild-type (red) and *sym1* mutants (blue). Abbreviations: *mitf* (*microphthalmia-associated transcription factor*), *dct* (*dopachrome tautomerase*).

mutants the developmental timing of chromatophore specification and migration is disrupted, but not the subsequent differentiation and proliferation of the progenitor cells.

Craniofacial cartilage defects in sym1 mutants

One of the strongest phenotypes of *sym1* mutant embryos and larvae is the abnormal size and shape of the jaws (Figs. 2C, D). The embryonic zebrafish head skeleton is derived from three initial streams of cranial neural crest cells (Schilling and Kimmel, 1994) that form the first (mandibular) and second (hyoid) arches, and ceratobranchials I–V. In *sym1* mutants, Alcian blue staining revealed that Meckel's cartilage was displaced ventrally, the ethmoid plate did not form due to incomplete fusion of the trabeculae, and the hyosymplectic and ceratohyal cartilage structures were either reduced in size or missing altogether (Figs. 3A–D). Also, while the jaw structures were always abnormal in *sym1* mutants, the severity of the cartilage defects depended on their position along the A/P axis. For example, the 1st arch derivatives were always present but, the 2nd arch derivatives were missing in 60% (n = 50) of the mutants, while the ceratobranchial arches were always completely absent (Figs. 3A, C).

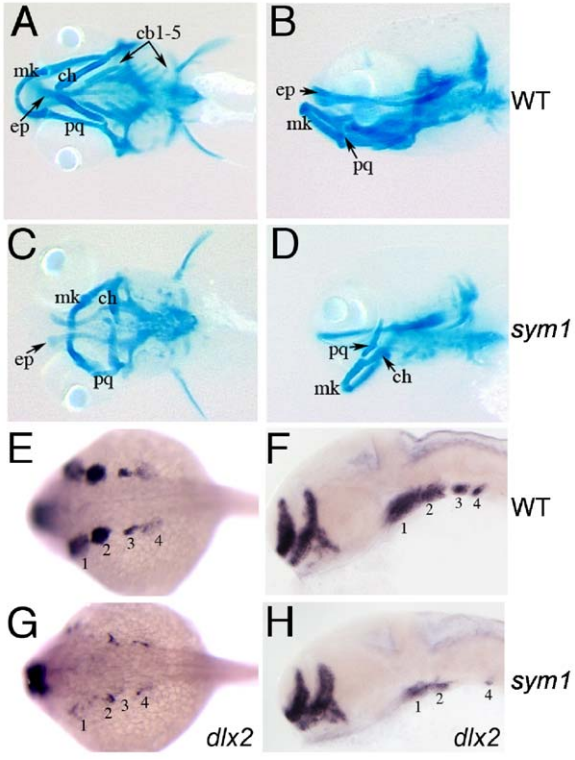

Fig. 3. Abnormal pharyngeal arch development in *sym1* mutants. Wild-type (A, B) and *sym1* mutant (C, D) embryos at 5 dpf, stained with Alcian blue to reveal craniofacial cartilages. Ventral (A, C) and lateral (B, D) views show that the 1st (mk) and 2nd (ch) arch derivatives are present but abnormal in *sym1* mutants, whereas 3rd arch-derived cartilages (cb1–5) are missing altogether. *dlx2* expression in migrating neural crest pharyngeal arch precursors, shown in dorsal views at 24 hpf in wild-type (E) and *sym1* mutant (G) embryos, and in lateral views of 32 hpf wild-type (F) and *sym1* mutant (H) embryos. *sym1* mutants have reduced *dlx2* expression in migrating neural crest cells that generate the 1st and 2nd arch derivatives (labeled 1 and 2), and more severely reduced *dlx2* expression in neural crest cells that generate the pharyngeal cartilages (labeled 3 and 4; G, H). Abbreviations: Meckel's cartilage (mk), palatoquadrate (pq), ceratohyal arch (ch), ethmoid plate (ep), and ceratobranchial (cb) arches 1–5.

The *dlx2* gene is required for jaw development and is expressed by neural crest cells that contribute to the pharyngeal arches as well as by migratory arch-associated neural crest cells (Figs. 3E–H, also Akimenko et al., 1994; Schilling and Kimmel, 1997). In *sym1* mutant embryos, *dlx2* expression was markedly reduced at 24 hpf in all recognizable arch-associated regions, especially the third arch, where *dlx2* staining was absent (Fig. 3G). A similar *dlx2* expression pattern was observed at 32 hpf (Fig. 3H). Reduced *dlx2* expression correlates with the severity of cartilage defects, as neural crest cells in the posterior arch regions give rise to more posterior cartilage elements, such as the ceratobranchials (Schilling and Kimmel, 1994), which are absent in *sym1* mutant embryos. Lastly, the expression of *sox9a* in the arches of *sym1* mutant embryos at 24 hpf and 48 hpf was also reduced (Suppl. Fig. 1), consistent with the reduction of *dlx2* expression.

The sym1 mutation inactivates the zebrafish foxd3 gene

Genetic linkage analysis of the *sym1* phenotype to 239 microsatellite markers revealed that markers z5294 and z10183 were within 1–2 cM from the *sym1* mutation on chromosome 6 (Fig. 4A). Because *sym1* mutants had severe defects in neural crest-derived sympathetic neurons and cranial cartilages, we searched the available zebrafish meiotic, radiation hybrid, and heat-shock maps within this region, to identify ESTs and cloned genes expressed in developing neural crest. The most promising candidate gene was *foxd3*, a member of the forkhead family of transcription factors (Odenthal and Nusslein-Volhard, 1998) and a marker of premigratory neural crest cells (Kelsh et al., 2000; Odenthal and Nusslein-Volhard, 1998). *foxd3* resides within 1 cM from the z10183 marker in the zebrafish radiation-hybrid mapping panels (Fig. 4A, http://zfin.org). The genomic sequence harboring the single *foxd3* coding exon was determined, and primers flanking this region were used to amplify genomic DNA from the *sym1* heterozygous F2 parents, as well as F3 homozygous mutant and wild-type embryos. Alignment of these DNA sequences identified a single guanine nucleotide deletion that induces a frame shift and a premature stop-codon within the DNA-binding domain of *foxd3* (Fig. 4B).

As a transcription factor of the winged-helix class, Foxd3 contains a helix–turn–helix core of three α-helices, flanked by two loops, or "wings", within the DNA-binding domain (Carlsson and Mahlapuu, 2002). The third helix contacts the major groove, while the second (most C-terminal) winged region binds to the phosphate backbone in the minor groove, conferring DNA recognition specificity; this region also contains a highly conserved stretch of 16 amino acids representing the nuclear localization signal (NLS) (Hellqvist et al., 1998). The *sym1* mutation predicts a loss of the second winged domain, abolishing the ability of the residual N-terminal peptide to bind DNA, as well as a loss of the NLS and C-terminal transcriptional effector domain (Fig. 4B, also Pani et

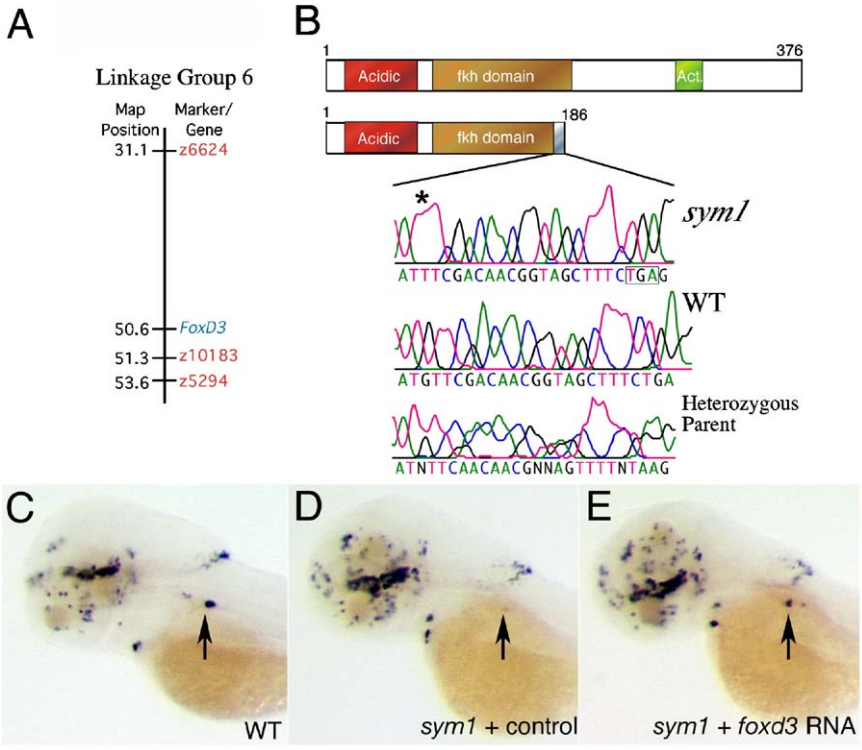

Fig. 4. *sym1* is an inactivating mutation in *foxd3*. (A) Linkage of the *foxd3* gene to the CA repeat markers on zebrafish chromosome 6. The positions of markers z10183, z6624 and z5294, are highlighted in orange (source http://zfin.org), while *foxd3* is highlighted in blue. The z10183 marker was mapped to within 1 cM of the *foxd3* gene. (B) Schematic diagrams of the wild-type and mutant Foxd3 proteins. In *sym1*, a guanine (537) deletion results in a frame shift leading to a premature stop codon and disruption of the encoded DNA-binding domain. An acidic domain is highlighted in orange at the N-terminus, and the C-terminus transcriptional effector domain is shown in green. Chromatogram traces below the schematic illustrate the nucleotide change (asterisk) affecting the *foxd3*-coding region. (C–E) Injection of *foxd3* RNA rescues the sympathetic *th*-expression pattern in *sym1* mutant embryos. Dorso-lateral views at 4 dpf of wild-type (C) and *sym1* mutant embryos (D, E) labeled with the *th* riboprobe. Wild-type siblings contain 10–40 *th*-expressing cells in the cervical complex at this stage (C), whereas the *sym1* mutant embryos injected with control RNA have 0–2 *th*-expressing cells (D). Injection of full-length *foxd3* RNA into *sym1* mutant embryos results in rescue (E), defined as >10 *th*-expressing sympathetic neurons in the region of the cervical complex. Arrows indicate position of the cervical complex.

al., 1992). The recessive nature of the *sym1* mutant phenotype, together with the loss of critical functional domains, predicts that *sym1* is a functional null allele of zebrafish *foxd3*.

To confirm that the *foxd3* gene was responsible for the *sym1* phenotype, we transcribed full-length, wild-type *foxd3* RNA in vitro and injected it into one cell-stage embryos from *sym1* heterozygous parents. These embryos, together with control RNA-injected embryos, were analyzed for the rescue of sympathetic neurons based on *th* expression (Figs. 4C–E). *foxd3* mRNA rescued the *th* expression pattern in the sympathetic cervical complex, defined as >10 *th*-positive sympathetic neurons at 4 dpf, in 83% of the injected *sym1* mutant embryos ($n = 24$). The number of *th*-positive neurons in *sym1* control-injected embryos was identical to that of uninjected *sym1* embryos (Figs. 4C–E). To show that the specific loss of *foxd3* function leads to the *sym1* phenotype, we injected one-cell stage embryos with morpholino phosphorodiamidate oligonucleotides targeting the translation start site of *foxd3*. Injection of 20 ng/embryo was sufficient to specifically phenocopy the peripheral sympathetic nervous system and cartilage defects of *sym1* mutants (data not shown). Notably, melanophore development appeared normal in injected embryos, even at very high concentrations (35–50 ng/embryo). Together, these experiments demonstrate that disruption of the *foxd3* gene is responsible for the selective neural crest phenotypes observed in *sym1* mutant embryos.

Normal somite and floor plate development in sym1 mutants

During zebrafish embryonic development, *foxd3* is expressed by floor plate cells and later in the developing somites (Odenthal and Nusslein-Volhard, 1998). In *sym1* mutant embryos, somite development appeared normal at all stages examined (1–5 dpf) in terms of the timing and number of somite pairs that developed, as well as somite size and shape (Figs. 2A, B; data not shown). The somitic expression of *myoD* was also indistinguishable between *sym1* mutants and wild-type siblings (Suppl. Figs. 2A, D), as was the pattern of floor plate expression of *twhh* and *col2a* (Suppl. Figs. 2B, C, E, F). Based on these findings, we conclude that *foxd3* is not normally required for somite or floor plate development in zebrafish.

foxd3 function is required for the selective specification of early neural crest cell subpopulations

To understand the contribution of *foxd3* function to neural crest development, we studied *sym1* mutants for the expression of *tfap2a*, *snai1b* and *sox10* transcription factors, which are

coexpressed in neural crest cells with *foxd3* in wild-type embryos and play important roles in early neural crest development (Barrallo-Gimeno et al., 2004; Dutton et al., 2001; Gammill and Bronner-Fraser, 2003; Knight et al., 2003; Thisse et al., 1995). *crestin* (*ctn*) was used as a pan-neural crest marker (An et al., 2002; Luo et al., 2001; Rubinstein et al., 2000). At the 3- to 5-somite stages, neural crest progenitors were present in the neural plate border in the anterior portion of embryos (Figs. 5A–E). The number of neural crest progenitors expressing *foxd3* and *tfap2a* were the same in both *sym1* and wild-type embryos (compare Figs. 5A, B with 5F, G), whereas expression of the *snai1b* and *sox10* transcription factors at the neural plate border was strongly reduced in *sym1* mutants (Figs. 5H, I), as was the expression of *crestin* (Fig. 5J). These differences in gene expression levels persisted through the 10-somite stage, with decreased expression of *sox10*, *snai1b* and *crestin* becoming more pronounced and more apparent in both cranial and nascent trunk neural crest (Suppl. Fig. 3). The cranial neural crest expression of *foxd3* in wild-type embryos normally begins to decrease at the 10-somite stage; however, *sym1* mutants continued to show robust cranial expression of *foxd3* (Suppl. Fig. 3). Therefore, to determine if the loss of *sox10*, *snai1b* and *crestin* expression corresponds to the loss of premigratory neural crest cells, we counted the number of *foxd3*-positive cells in wild-type and *sym1* mutants at the 12-somite stage. Wild-type embryos contained an average of 44.5 such cells in this region, while *sym1* mutants had an average of 45.3 ($n = 8$, $p > 0.73$). Furthermore, the midline convergence of the neural plate borders and formation of the premigratory neural crest population was not developmentally delayed in *sym1* mutant embryos (Suppl. Fig. 4). These results suggest that early induction of the neural crest cell population at the neural plate border occurs normally, based on the expression of *tfap2a* and *foxd3,* but that fewer of these cells express normal levels of *sox10*, *snai1b* and *ctn* in *sym1* mutants compared to wild-type embryos.

The lineage-specific defects and abnormal gene expression patterns observed in *sym1* mutants suggests that *foxd3* is differentially required for the specification and/or survival of a subset of the neural crest sublineages. Zebrafish harboring mutations in *tfap2a* and *sox10* also show selective defects in a subset of neural crest derivatives, suggesting that they also play critical roles during neural crest specification and development (see Discussion). Thus, we analyzed *tfap2a*, *sox10* and *snai1b* expression during neural crest specification, between the 10- to 12-somite stages (Fig. 6) and followed the expression throughout later stages (Supp. Fig. 5). In wild-type embryos at the 10- to 12-somite stage, the transcription factors *tfap2a*, *sox10* and *snai1b* are normally expressed in both premigratory and migratory neural crest cells (Fig. 6). The expression of *tfap2a* (Figs. 6D–F) and *sox10* (Figs. 6J–L) was reduced in both the cranial and trunk neural crest of *sym1* mutant embryos, with more severe defects seen in trunk neural crest expression. In contrast, the expression of *snai1b* was severely reduced throughout the neural crest in *sym1* mutant embryos, at all stages examined (Figs. 6M–R; Suppl. Fig. 5). Therefore, while *snai1b* expression appears be the most sensitive to the loss of *foxd3* function, normal expression of *sox10* and *tfap2a* is also dependent on *foxd3* activity, particularly during the period when neural crest specification is occurring, at the 10- to 12-somite stage.

The analysis of *snai1b*, *sox10* and *tfap2a* expression in *sym1* mutants revealed neural crest-specific defects in gene expression patterns, consistent with recent studies showing that *foxd3* functions in a cell-intrinsic manner during neural crest development (Cheung et al., 2005). For example, *sox10* expression was not affected in the developing otic placode in *sym1* mutants, even though this placode forms adjacent to the developing neural crest domain (compare Figs. 6H with K). Double ISH analysis confirmed that the reduced expression patterns were only associated with *foxd3*-expressing cells (data not shown). Furthermore, examination of Rohon–Beard sensory neuron development showed that other cell types generated at the neural plate border are not affected in *sym1* mutants (Suppl. Fig. 4). Likewise, expression of *sox2* and *msxb* at the neural plate border did not differ between *sym1* mutant and wild-type embryos (Suppl. Fig. 4). These results suggest

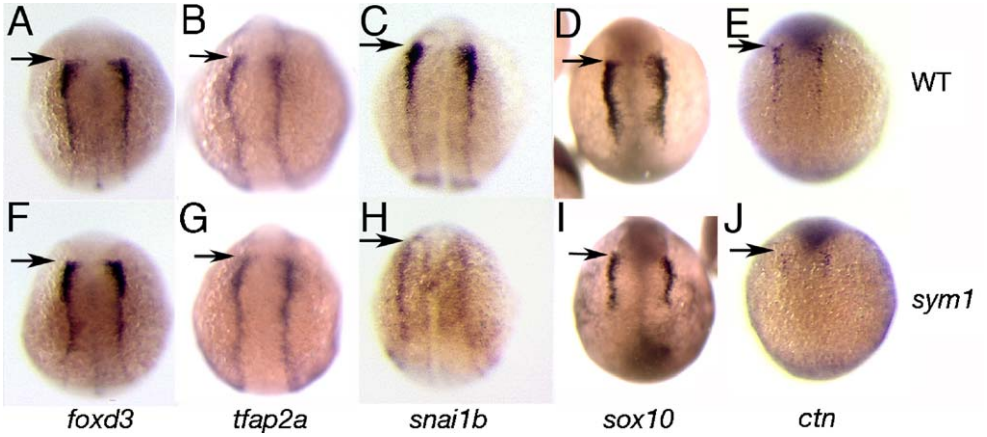

Fig. 5. Molecular defects in neural crest specification in *sym1* mutants. Dorsal views of wild-type (A–E) and *sym1* mutant (F–J) embryos. Neural plate border expression of *foxd3* (A, F), *tfap2a* (B, G), *snai1b* (C, H), *sox10* (D, I) and *ctn* (*ctn* E, J) in 3-somite-stage embryos. Decreased expression of *sox10*, *snai1b* and *ctn*, but not *foxd3* and *tfap2a* is evident in *sym1* mutants. Arrows indicate position of midbrain–hindbrain boundary.

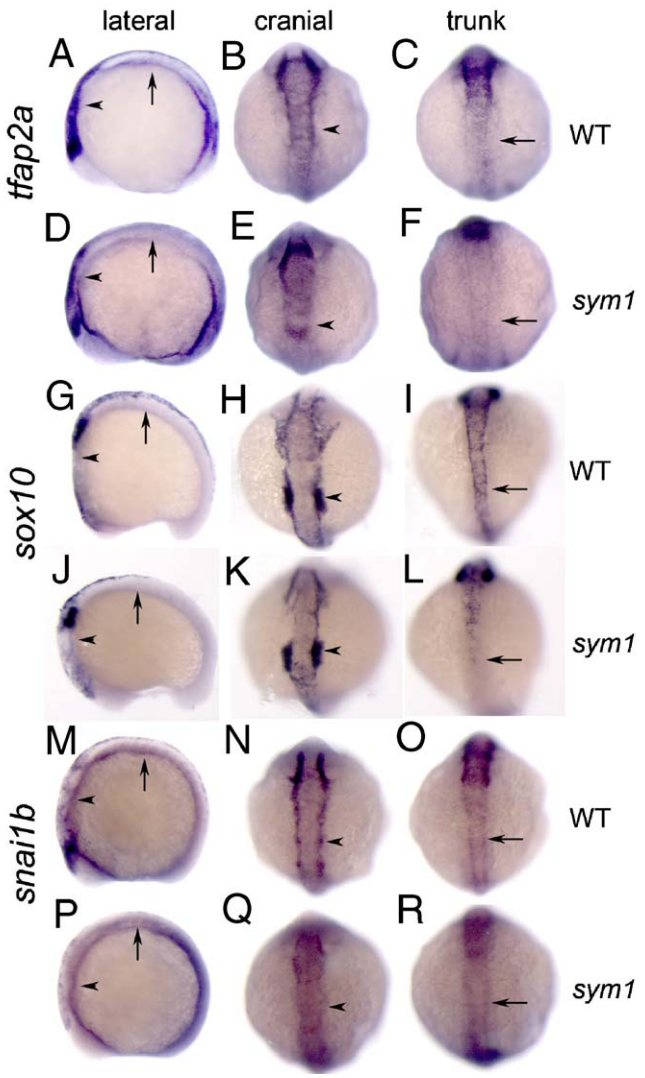

Fig. 6. Gene expression abnormalities in premigratory and early migrating neural crest cells in *sym1* mutants. Lateral, cranial and trunk views of wild-type (A–C, G–I, M–O) and *sym1* (D–F, J–L, P–R) embryos, showing expression of *tfap2a* (A–F), *sox10* (G–L), and *snai1b* (M–R) at the 10-to 12-somite stage. *tfap2a* expression begins to decrease in *sym1* mutants at this stage, particularly in the trunk (compare A, C with D, F). The expression of *sox10* in *sym1* mutants (J–L) and *snai1b* (P–R) is reduced in both cranial and trunk neural crest. The reduction in *sox10* expression is specific to the neural crest because *sox10* expression in the developing otic placode (arrowheads) is normal in wild-type and *sym1* mutants (compare H with K). Arrows indicate the position of the trunk neural crest.

that the developmental requirement for *foxd3* function is specific to the developing neural crest. Thus, induction of the neural plate and the generation of neural crest progenitors as well as the premigratory neural crest population appears to occur normally in *sym1* mutants, but the normal transcription factor program within these cells is severely disrupted.

Neural crest migration defects in sym1 mutants

The active migration of cranial neural crest in wild-type zebrafish embryos occurs in three distinct streams, emerging from rhombomeres (r) r2, r4 and r6 and migrating to the mandibular (1), hyoid (2), and posterior (3) arches, respectively (Schilling and Kimmel, 1994), which can be easily visualized with the pan-neural crest marker *ctn* (Figs. 7A, B). At the 12-somite stage, *sym1* mutants showed a reduction in *ctn*-positive cells contributing to the 1st stream, and almost no *ctn*-positive cells in the 2nd stream (Figs. 7E, F, asterisk). In contrast, the number of *ctn*-positive cells at the position of the developing 3rd cranial neural crest stream was only slightly reduced in *sym1* mutants at the 12-somite stage relative to their wild-type siblings (Figs. 7E, F). Analysis of *foxd3* expression in *sym1* mutants at the 12-somite stage revealed that normal numbers of premigratory cranial neural crest cells were present, but failed to express *ctn* or properly migrate away from the dorsal neural tube (compare Figs. 7E with G). This analysis also revealed that *sym1* mutants continued to express *foxd3* at very high levels in the cranial neural crest, at a time when expression of this gene is nearly extinguished in wild-type siblings (compare Figs. 7C, D with G, H).

Double ISH analysis of *foxd3* and *ctn* expression in *sym1* mutants detected *ctn* expression once neural crest migration was initiated, at the 14-somite stage for the 1st stream and the 17-somite stage for the 2nd stream, corresponding to down-regulation of *foxd3* expression (Figs. 7I, J; data not shown). The most anterior cranial neural crest cells in *sym1* mutants, which contribute to formation of the olfactory placode (Whitlock, 2005), continued to express *foxd3* until the 26-somite stage but failed to express *ctn* (Figs. 7L, M. black arrowhead). At this stage, *ctn*-expressing neural crest cells were migrating to deep ventral regions in the head in wild-type embryos (Figs. 7I, J, black arrow), while in *sym1* mutants the migration pattern of the *ctn*-positive cells was disrupted: although some cells did move laterally over the head, they failed to migrate deeper into more ventral head structures (Figs. 7L, M, black arrow).

Analysis of the trunk neural crest cells in *sym1* mutants revealed similar defects in the initiation and pattern of neural crest migration. For example, in the trunk at the 26-somite stage, there was a significant delay (3–4 h) in the onset of migration, with only a small number of *ctn*-expressing cells migrating within the most anterior somites, similar to the migration delay observed for *mitf*-expressing cells (compare Figs. 2 and 7). Study of the *sox10* gene, which is also expressed in migrating trunk neural crest cells (Dutton et al., 2001), showed a similar delay in neural crest migration in *sym1* mutants at the 26-somite stage, consistent with coexpression of these genes in migrating trunk neural crest cells (Figs. 7O, P; data not shown). A comparison of *ctn*-expressing trunk neural crest cells in transverse sections of *sym1* mutant and wild-type embryos revealed that the vast majority of *sym1* mutant neural crest cells remained localized between the dorsal surface of the neural keel and overlying ectoderm (Figs. 7K–N).

In zebrafish, most trunk neural crest cells are lineage-restricted and migrate along two stereotypical pathways (Raible and Eisen, 1994). Early migrating neural crest cells migrate medially between the neural tube and somite (Fig. 7K, arrow), and generate a number of cell types, including neurons, glia and pigment cells. In contrast, neural crest cells migrate later along a lateral pathway and typically generate pigment cells (Fig. 7K,

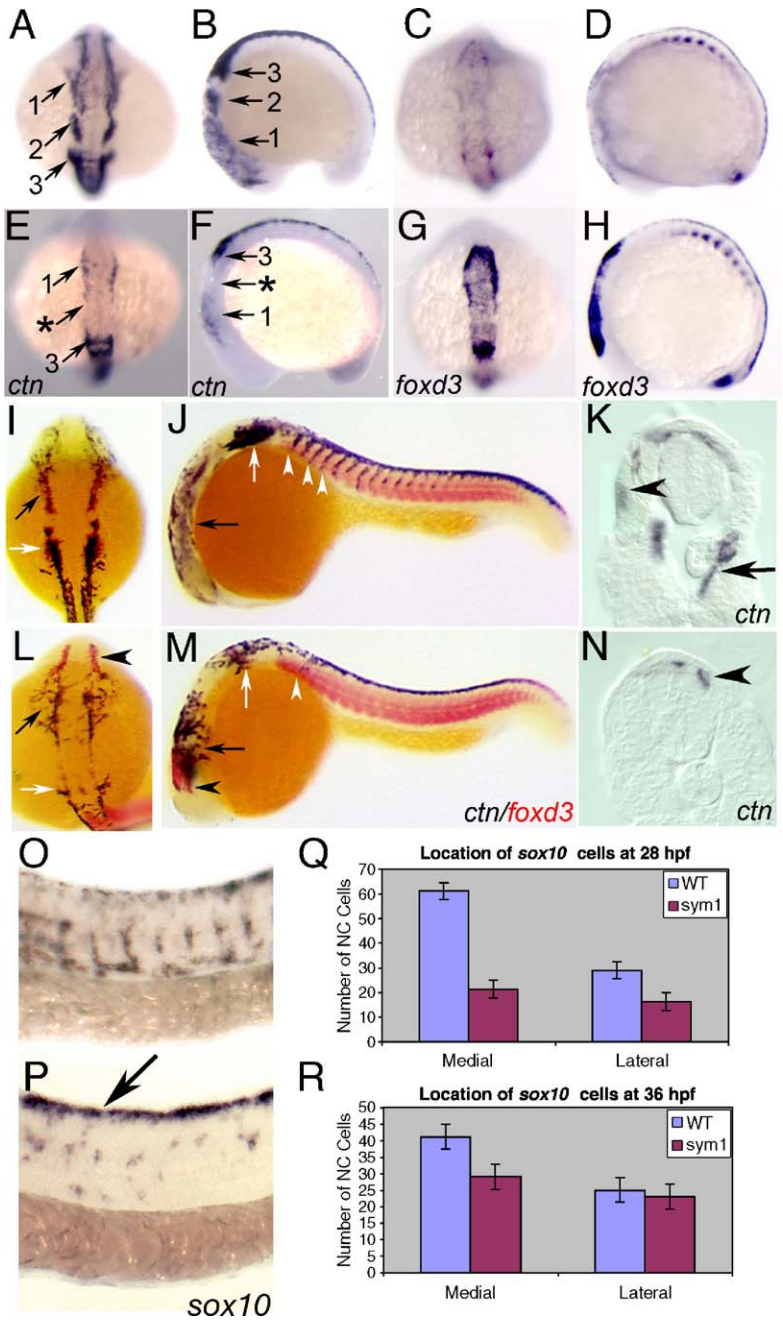

Fig. 7. Abnormal cell migration in *sym1* mutant embryos. Wild-type (A–D) and *sym1* mutant (E–H) embryos at the 12-somite stage, showing dorsal (A, E, C, G) and lateral (B, F, D, H) views. *ctn* expression reveals migration of the three cranial neural crest streams in wild-type embryos (A–B, numbered arrows). In *sym1* embryos, *ctn* expression in cranial neural crest is severely reduced in the 1st neural crest stream (E, F) and almost absent in the 2nd stream (arrow with asterisk in E, F). *ctn*-positive cells of the 3rd stream are present in *sym1* mutants, but only a few cells migrate ventrally (compare F with B). At the same stage, *foxd3* expression is normally rapidly downregulated in wild-type embryos upon migration (C–D), but persists in *sym1* mutants (G–H), showing that the cranial premigratory crest is present, but does not migrate. Wild-type (I–J) and *sym1* mutant (L–M) embryos double labeled with *ctn* (black) and *foxd3* (red) at the 26-somite stage, showing dorsal (I, L) and lateral (J, M) views. At this stage, *ctn* is expressed throughout the head in deep ventral positions of wild-type embryos (I, J, black arrow); however, in *sym1* mutants, *ctn*-positive cells fail to migrate ventrally, and spread out more laterally (L, M, black arrow). The expression of *ctn* is also strongly reduced in the region of the hindbrain posterior to the otic vesicle in *sym1* mutants (L–M, white arrows), while *foxd3* expression remains high in the anterior-most neural crest cells (L, M, black arrowhead). Numerous, *ctn*-expressing trunk neural crest cells are seen migrating in wild-type embryos at the 26-somite stage (J; white arrowhead), but few *ctn*-positive cells are seen in *sym1* embryos (M; white arrowhead). Transverse sections at the anterior trunk level of 24 hpf wild-type (K) and *sym1* mutant (N) embryos, showing *ctn* expression in both dorsal-laterally (K, arrowhead) and medial (K, arrow) migrating neural crest cells in wild-type embryos. In *sym1* mutants, migration of *ctn*-expressing cells are delayed, and found only in dorsal positions at this stage (N, arrowheads). Lateral views of *sox10*-expressing neural crest cells in wild-type (O) and *sym1* (P) embryos at 24 hpf. In wild-type embryos, robust *sox10* expression is evident in migrating neural crest cells; however, in *sym1* mutants most of the *sox10*-expressing cells are still on the dorsal neural tube (P, arrow). Quantitation of *sox10*-positive cells located along each migration pathway at 28 hpf (Q) and 36 hpf (R) in wild-type (blue) and *sym1* mutants (red), shows that migration along the medial pathway is more severely affected in *sym1* mutants.

arrowhead). The analysis of both *sox10* and *ctn* expression at the 26-somite stage in *sym1* mutants showed a delay in the migration of cells along the medial pathway (Figs. 7K, N, O, P; data not shown). Therefore, we analyzed trunk neural crest migration along each pathway at later developmental stages to determine if the medially migrating neural crest cells continue to be affected in *sym1* mutants. By counting the numbers of *sox10*-expressing trunk neural crest cells during development, we found a 60% reduction in the number of cells along the medial pathway in *sym1* mutants at 28 hpf (Figs. 7O, P, Q). The number of cells migrating dorso-laterally was also reduced by 40% in *sym1* mutants at this stage (Fig. 7Q). However, by 48 hpf, the numbers of cells migrating along the lateral pathway had recovered to wild-type levels, whereas the number of medially migrating cells was still reduced by 29% in *sym1* mutants (Fig. 7R). Because cells migrating along the lateral pathway are chromatophore precursors, not neural precursors, we also counted the numbers of *dct*-expressing melanoblasts along both migration pathways at 36 hpf in *sym1* mutants. The results showed a pattern similar to the migrating *sox10*-expressing cells; the number of *dct*-positive cells migrating along the medial pathway was reduced by 20% in *sym1* mutants and no reduction was found for cells migrating along the lateral pathway (data not shown). Thus, the migration defect seen in *sym1* mutants appears to selectively affect the neural crest cells migrating along the medial pathway, which include the neuronal and glial precursors, and is consistent with the reduced numbers of migrating neuronal precursors that express *phox2b* and *zash1a* (Figs. 1G, H).

Loss of foxd3 function in sym1 mutants causes localized neural crest cell death

In *sym1* mutants, the *ctn* expression observed in the vagal neural crest at the 10-somite stage is severely reduced by 24 hpf (compare Figs. 7I with L, white arrow). The loss of these cells during development was investigated by TUNEL analysis to detect apoptotic cells. Between the 10–15 hpf stages, there were no significant differences in cell death between *sym1* and wild-type embryos, consistent with the correct numbers of presumptive neural crest cells being formed in *sym1* mutants at this time. However, beginning at 15 hpf the number of TUNEL-positive cells increased dramatically in the dorsal ectoderm of *sym1* mutant embryos within the region of the hindbrain, corresponding to the position of the developing 3rd neural crest stream (Fig. 8). Neural crest cell death in this region of *sym1* embryos was complete by 18 hpf, after which the number of TUNEL-positive cells in *sym1* returned to wild-type levels. To confirm that these dying cells were the *ctn*-positive neural crest cells lost in *sym1* mutants at later stages, we performed double labeling with *ctn* and TUNEL (Figs. 8C, F). The results show that at least some of these cells are neural crest cells, even though the expression of *ctn* is downregulated in *sym1* mutant embryos at this stage (see above). The numbers of TUNEL-positive cells did not differ in regions other than those containing neural crest cells in the dorsal ectoderm. The appearance of the TUNEL-positive cells correlates with the decreased numbers of *ctn*-positive cells at this time, and may contribute to the defects in the tissue derivatives normally arising from the 3rd neural crest stream in *sym1* mutants. Thus, *foxd3* is required for the survival of a subpopulation of neural crest cells in the hindbrain that normally gives rise to neurons, glia and the pharyngeal arches, all of which are severely affected in *sym1* mutants.

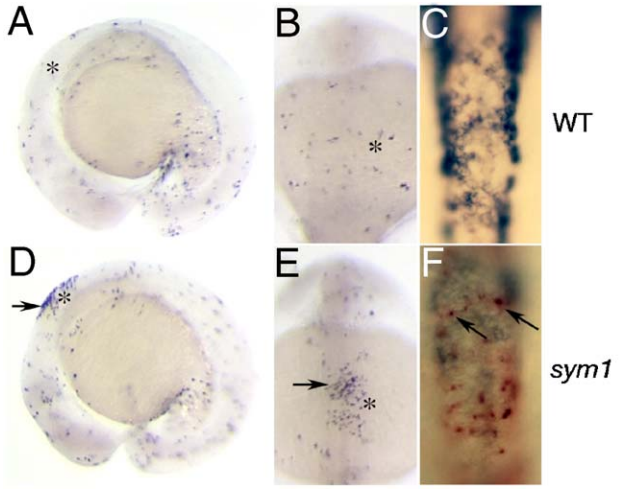

Fig. 8. Neural crest cell death in *sym1* mutants. Lateral (A, D) and dorsal (B, C, E, F) views of TUNEL labeled 15-somite stage wild-type (A–C) and *sym1* mutant (D–F) embryos shows an increase in dorsal TUNEL-positive cells in the hindbrain region in *sym1* mutants (arrows in D, E). Asterisks indicate the position of the developing otic placode. (C, F) Double labeling analysis with *ctn* (dark blue) and TUNEL (red) shows cell death in some neural crest cells that still express *ctn* in *sym1* mutants at this stage (arrows).

Discussion

In this study, we analyzed the first mutant isolated from our zebrafish peripheral sympathetic nervous system screen. The underlying mutation, designated *sympathetic mutation 1* (*sym1*), is a single nucleotide deletion that introduces a premature stop codon within the DNA-binding domain of zebrafish Foxd3, thus predicting a loss of DNA-binding activity. The ability of forced expression of wild-type zebrafish *foxd3* mRNA to rescue the *sym1* phenotype and successful phenocopying of the mutant using *foxd3*-specific antisense morpholinos provides strong confirmation of the specific loss of *foxd3* function. We show that functional *foxd3* is required for downregulating its own expression and is selectively required for sublineage fate specification, migration and survival. Our results indicate that *foxd3* functions by directing the expression of other essential transcription factors in nascent neural crest cell subpopulations and by promoting the survival of a subset of neural crest cells.

The role of foxd3 in early neural crest development

Previous studies in chickens and frogs have shown that forced misexpression of *foxd3* can activate neural crest marker genes, suggesting that it is required for the induction of neural crest. For example, the forced expression of *foxd3* in chick

neural epithelium can induce neural crest markers such as *Cad7*, the HNK1 epitope, Integrinβ1 and Laminin, while its expression in frog animal cap assays induces expression of *slug* and AP-2 (Cheung et al., 2005; Dottori et al., 2001; Pohl and Knochel, 2001; Sasai et al., 2001). While these studies indicate that *foxd3* is sufficient to induce neural crest gene expression, they do not address whether it is required for neural crest induction in vivo.

Our analysis of *sym1* mutants demonstrates that *foxd3* is not required for the initial stages of neural crest induction in zebrafish, because neural crest progenitors develop normally at the neural plate border in these mutants. Moreover, the correct numbers of early premigratory neural crest cells are generated in *sym1* mutants, and delaminate from the dorsal neural keel, indicating that the epithelial–mesenchymal transition does not require *foxd3* function. Our *sym1* mutant data are also consistent with recent findings by Cheung et al. (2005) showing that forced expression of *foxd3* in the neural epithelium of chick embryos does not interfere with the EMT process, but rather affects the subsequent migratory properties of the delaminated neural crest cells. Thus, the in vivo induction and generation of premigratory neural crest cells occur in a *foxd3*-independent manner.

Sublineage-specific fate determination by foxd3

In *sym1* mutants, there is a near complete loss of dorsal root ganglion, sympathetic and enteric neurons, and their precursor populations. The peripheral glia associated with the cranial ganglia and lateral line nerves are also severely reduced, and the normal re-expression of *foxd3* during later developmental stages is not observed. Since normal numbers of early premigratory cranial and trunk neural crest cells are present in *sym1* mutants, these data indicate that *foxd3* is required for the subsequent development of neuronal and glial progenitor cells of the neural crest. In contrast, melanocyte development is delayed in *sym1* mutants, while the number of differentiated cells at 5 dpf remains the same as wild-type. These results indicate that *foxd3* functions selectively to specify neuronal and glial sublineages, but is not required for specifying the later development of melanocytes or chromatophore lineages. In addition, analysis of the developing craniofacial skeleton in *sym1* mutants suggest that *foxd3* activity is also selectively required in different subpopulations of the cranial neural crest that give rise to the different arch derivatives.

Studies with antisense morpholinos directed against *foxd3* in cultured chick neural crest also show that different neural crest populations are sensitive to loss of *foxd3* function (Kos et al., 2001). For example, *foxd3* can repress melanogenesis in chicks, consistent with the absence of *foxd3* expression in dorso-laterally migrating melanoblasts. In contrast, our results indicate that *foxd3* does not contribute either positively or negatively to melanogenesis in developing zebrafish, because we did not detect either a decrease or an increase in the number of differentiated melanocytes or a difference in the final number of cells expressing *dct* and *mitf* in developing melanoblasts in *sym1* mutants. Also, in contrast to findings in chick, *foxd3* is likely to be expressed in melanoblasts in mice (Hromas et al., 1999; Labosky and Kaestner, 1998). This discrepancy may reflect differences in the pattern and duration of neural crest *foxd3* expression in avian versus fish and mammalian embryos. Nonetheless, the results from chick and fish indicate that the loss of *foxd3* activity does not affect all neural crest cells, but instead promotes the specification of a subset of neural crest cell lineages, which may differ slightly among different vertebrate species.

Genetic mechanisms underlying differential specification of the neural crest by foxd3

Our genetic analysis suggests that *foxd3* may regulate specification of the neural crest through differential activation of other neural crest-specific transcription factors, such as *snai1b* and *sox10*. Indeed, our genetic data indicate that *foxd3* lies upstream of these genes in premigratory neural crest cells. This hypothesis is supported by previous genetic studies in zebrafish showing that *foxd3* expression in premigratory neural crest cells is relatively normal in *tfap2a* (*lockjaw*/*mont blanc*) and *sox10* (*colourless*) mutants, (Barrallo-Gimeno et al., 2004; Kelsh and Eisen, 2000; Knight et al., 2003). Also, consistent with *foxd3* affecting both *sox10*- and *tfap2a*-dependent genetic pathways, *sym1* mutants appear to display a more severe neural crest phenotype than either *sox10* or *tfap2a* mutants alone, with the exception of chromatophores (Barrallo-Gimeno et al., 2004; Elworthy et al., 2005; Kelsh and Eisen, 2000; Knight et al., 2003). Thus, a simple explanation for the absence of glia, as well as DRG, sympathetic and enteric neurons in *sym1* mutants is that the loss of *foxd3* expression reduces the number of both *tfap2a*- and *sox10*-expressing neural crest progenitors. Given that *snail/slug* family members can affect early neural crest development in other species, it remains possible that the reduction in *snai1b* expression in *sym1* neural crest subpopulations may also contribute to the observed neuronal and glial defects in these mutants. However, since *snai1b* mutants remain to be isolated in zebrafish, it has not been possible to test whether this gene also differentially regulates neural crest specification.

The relatively normal development of melanocytes and other chromatophores in *sym1* mutants may seem inconsistent with the reduced sizes of *sox10*-, *tfap2a*- and *snai1b*-expressing neural crest populations and with the chromatophore defects observed in *colourless* (*cls*) and *lockjaw/mont blanc* (*low*) mutants. In *cls* mutants, for example, melanophore and iridiphore sublineages are severely disrupted while xanthophore development persists (Dutton et al., 2001; Kelsh and Eisen, 2000) while in *low* mutants the development of all three chromatophore sublineages is affected (Barrallo-Gimeno et al., 2004; Kelsh and Eisen, 2000; Knight et al., 2003). This apparent discrepancy becomes less striking when one considers that in *sym1* mutants, neural crest subpopulations expressing *sox10* and *tfap2a* (and *snai1b*) are retained, albeit in significantly smaller sizes, and a small number of *sox10*-expressing neural crest precursors migrate normally. These observations suggest that the subpopulations of neural crest cells expressing *sox10* and *tfap2a* in *sym1* mutants may be

chromatophore progenitors and in these specific sublineages the expression of such genes may occur independently of *foxd3* function.

The differential requirements for *foxd3* function between neuronal and chromatophore sublineages gain significance in light of abundant evidence from studies in birds and mice indicating that the segregation of neuronal and pigment precursors is one of the earliest events in neural crest cell diversification (Frank and Sanes, 1991; Greenwood et al., 1999; Henion and Weston, 1997; Luo et al., 2003a; Perez et al., 1999; Reedy et al., 1998; Vogel and Weston, 1988; Wilson et al., 2004). In zebrafish, clonal analysis has demonstrated a clear distinction between neurogenic and melanogenic neural crest cells of the head (Schilling and Kimmel, 1994), and a strong clonal bias toward distinct neuronal and chromatophore progenitors in the trunk has been reported (Raible and Eisen, 1994). Our results suggest that *foxd3* plays a crucial instructive role, either directly or indirectly, in the establishment of neuronal neural crest sublineages. Indeed, the loss of *foxd3* function in *sym1* mutants does not result in the expansion of chromatophore sublineages, nor do neuronal lineages expand in *nacre/mitfa* mutants in the absence of melanophore progenitors (Dorsky et al., 2000; Lister et al., 1999). These observations suggest that the specification and segregation of these sublineages depend upon instructive signaling events and that neither represents a default developmental pathway.

foxd3 is differentially required for trunk neural crest cell migration

Our results also indicate that *foxd3* is normally required for regulating the overall migratory capacity of most neural crest cells and the timing of trunk neural crest migration. These findings agree with recent studies in chick showing that *foxd3* function is required for neural crest migration by regulating the expression of cell–cell adhesion molecules, such as N-cadherin (Cheung et al., 2005; Dottori et al., 2001; Nakagawa and Takeichi, 1998; Pietri et al., 2004). In chicks, at least some of these *foxd3* functions are mediated through *sox10*, consistent with the severe defects in trunk neural crest migration observed in *cls/sox10* zebrafish mutants (Cheung et al., 2005; Dutton et al., 2001; Kelsh and Eisen, 2000). Thus, the reduced expression of *sox10* may account for some of the neural crest migration defects observed in *sym1* mutants. However, we also show that loss of *foxd3* function has more pronounced effects on neural crest cells migrating along the medial pathway, whereas *cls* mutants have more severe defects in neural crest cells migrating along the lateral pathway (Dutton et al., 2001; Kelsh and Eisen, 2000). Thus, other genes may function downstream of *foxd3* to mediate *foxd3*-dependent neural crest migration. Likely candidates are the *snail* family of transcription factors, which regulate the migration of a number of cell types, including neural crest cells, during development and disease (Aybar et al., 2003; Carl et al., 1999; Cheung et al., 2005; Gupta et al., 2005). Indeed, analysis of the expression of early neural crest markers in *sym1* mutants showed *snai1b* levels in neural crest cells is the most severely reduced. Thus, *foxd3* and *snai1b* may function together in the premigratory neural crest to induce migration of cells along the medial path. Interestingly, the position and intensity of *snai1b* labeling in the premigratory crest cells of *cls* mutants was indistinguishable from wild-type embryos (Kelsh and Eisen, 2000), further suggesting that activation of *snai1b* may be necessary to promote migration of trunk neural crest cells along the medial pathway.

While migration defects may contribute to the loss of neurons in *sym1* mutants, unimpeded neuronal differentiation in other mutants in which most neural crest cells fail to disperse from the dorsal neural tube (e.g., *spadetail* and *colgate*; Ignatius, Nambiar and Henion, unpublished data) suggests that the differentiation of these cells may be independent of their ability to migrate. This notion is strengthened by the presence of well-differentiated melanocytes along the dorsal stripe in *sym1* mutants, indicating that some melanoblast precursors (presumably the sub-population that travels along the medial pathway) are able to differentiate even though they fail to migrate. Thus, *foxd3* function during neural crest specification may temporally precede or coincide with trunk neural crest migration.

Molecular specification, patterning and survival of the cranial neural crest by foxd3

In *sym1* mutants, the anterior mandibular and hyoid elements of the craniofacial skeleton were less affected than the posterior branchial arches, which were nearly absent, suggesting a differential requirement for *foxd3* function in patterning the cranial neural crest. Consistent with this hypothesis, precursors in the 3rd arch that generate the branchial arch elements exhibit the strongest defects in *dlx2* and *sox9a* expression and migration (Aybar et al., 2003; Carl et al., 1999; LaBonne and Bronner-Fraser, 2000). Analysis of *cls* mutants suggests that *sox10* is not required for ectomesenchymal crest development in the head (Kelsh and Eisen, 2000), so the reduced expression of *sox10* in *sym1* mutants is unlikely to cause these defects. In contrast, mutations in *tfap2a* cause severe reductions in cartilage elements generated from the 2nd and 3rd arch streams, similar to findings in *sym1* mutants (Barrallo-Gimeno et al., 2004; Knight et al., 2003). Thus, the reduction of *tfap2a* expression in the cranial neural crest of *sym1* mutants supports the idea that *foxd3* functions through *tfap2a* to specify and generate the craniofacial skeleton. However, the early expression of *tfap2a* in the cranial neural crest (before the 10-somite stage) is independent of *foxd3* function, so it is also possible that *tfap2a* functions independently of *foxd3* during craniofacial development. Furthermore, it was recently shown that *sox9a* and *sox9b* play essential and synergistic roles in the patterning and development of the craniofacial skeleton in zebrafish (Yan et al., 2005). These results showed that *sox9* genes regulate *foxd3* but not *tfap2a* expression in pharyngeal arch cells. Thus, it appears that the correct patterning of the pharyngeal arches may depend upon regulated interactions among the *tfap2a*, *sox9a/b* and *foxd3* pathways.

The striking loss of the branchial arches, neurons and glia in *sym1* mutants may also result from the specific loss of hindbrain premigratory neural crest cells by cell death, consistent with the

severe loss of *crestin*-positive cells in the hindbrain at 24 hpf. The regulation of cell death by *foxd3* may be a conserved function, because disruption of this gene in mice revealed an essential role in embryonic stem cell survival (Hanna et al., 2002). The downstream effectors of *foxd3*-mediated cell death are not known, but our studies suggest that members of the *Snail* family of transcriptional repressors are possible candidates. Indeed, recent studies have shown that *Snail* family members act as survival factors in progenitor cell populations and are overexpressed in a number of human cancers (Barrallo-Gimeno and Nieto, 2005; Gupta et al., 2005; Inoue et al., 2002; Wu et al., 2005). Thus, the loss of *snai1b* expression in the neural crest progenitor cells in *sym1* mutants may account for the inappropriate cell death observed in the premigratory neural crest at the 15-somite stage. Determining the genetic pathways downstream of *foxd3* in neural crest development may therefore provide insights into how this transcription factor regulates cell death in other progenitor populations in both development and disease.

Acknowledgments

We thank R. Segal, D. Rowitch, D. Fisher and Qiufu Ma for critically reading the manuscript, L. Zon for the F1 WIK ENU females and our many colleagues for numerous plasmids. We thank Jen Rhodes, Teresa Palomero, John Morris and Cicely Jette for help with the early pressure zebrafish mutagenesis and Juan Gao and Nicolas Campisi for excellent technical assistance. This work was supported by grants from the NIH, CA104605 to A.T.L. and NS38115 to P.D.H. R.S. is supported by a Hope Street Kids Foundation fellowship.

Appendix A. Supplementary data

Supplementary data associated with this article can be found in the online version at doi:10.1016/j.ydbio.2005.12.035.

References

Akimenko, M.A., Ekker, M., Wegner, J., Lin, W., Westerfield, M., 1994. Combinatorial expression of three zebrafish genes related to distal-less: part of a homeobox gene code for the head. J. Neurosci. 14, 3475–3486.

Allende, M.L., Weinberg, E.S., 1994. The expression pattern of two zebrafish achaete–scute homolog (ash) genes is altered in the embryonic brain of the cyclops mutant. Dev. Biol. 166, 509–530.

An, M., Luo, R., Henion, P.D., 2002. Differentiation and maturation of zebrafish dorsal root and sympathetic ganglion neurons. J. Comp. Neurol. 446, 267–275.

Aybar, M.J., Nieto, M.A., Mayor, R., 2003. Snail precedes slug in the genetic cascade required for the specification and migration of the *Xenopus* neural crest. Development 130, 483–494.

Barrallo-Gimeno, A., Nieto, M.A., 2005. The Snail genes as inducers of cell movement and survival: implications in development and cancer. Development 132, 3151–3161.

Barrallo-Gimeno, A., Holzschuh, J., Driever, W., Knapik, E.W., 2004. Neural crest survival and differentiation in zebrafish depends on mont blanc/tfap2a gene function. Development 131, 1463–1477.

Bisgrove, B.W., Raible, D.W., Walter, V., Eisen, J.S., Grunwald, D.J., 1997. Expression of c-ret in the zebrafish embryo: potential roles in motoneuronal development. J. Neurobiol. 33, 749–768.

Carl, T.F., Dufton, C., Hanken, J., Klymkowsky, M.W., 1999. Inhibition of neural crest migration in *Xenopus* using antisense slug RNA. Dev. Biol. 213, 101–115.

Carlsson, P., Mahlapuu, M., 2002. Forkhead transcription factors: key players in development and metabolism. Dev. Biol. 250, 1–23.

Cheung, M., Chaboissier, M.C., Mynett, A., Hirst, E., Schedl, A., Briscoe, J., 2005. The transcriptional control of trunk neural crest induction, survival, and delamination. Dev. Cell 8, 179–192.

Chiang, E.F., Pai, C.I., Wyatt, M., Yan, Y.L., Postlethwait, J., Chung, B., 2001. Two sox9 genes on duplicated zebrafish chromosomes: expression of similar transcription activators in distinct sites. Dev. Biol. 231, 149–163.

Dorsky, R.I., Raible, D.W., Moon, R.T., 2000. Direct regulation of nacre, a zebrafish MITF homolog required for pigment cell formation, by the Wnt pathway. Genes Dev. 14, 158–162.

Dottori, M., Gross, M.K., Labosky, P., Goulding, M., 2001. The winged-helix transcription factor Foxd3 suppresses interneuron differentiation and promotes neural crest cell fate. Development 128, 4127–4138.

Dutton, K.A., Pauliny, A., Lopes, S.S., Elworthy, S., Carney, T.J., Rauch, J., Geisler, R., Haffter, P., Kelsh, R.N., 2001. Zebrafish colourless encodes sox10 and specifies non-ectomesenchymal neural crest fates. Development 128, 4113–4125.

Ekker, S.C., Ungar, A.R., Greenstein, P., von Kessler, D.P., Porter, J.A., Moon, R.T., Beachy, P.A., 1995. Patterning activities of vertebrate hedgehog proteins in the developing eye and brain. Curr. Biol. 5, 944–955.

Elworthy, S., Pinto, J.P., Pettifer, A., Cancela, M.L., Kelsh, R.N., 2005. Phox2b function in the enteric nervous system is conserved in zebrafish and is sox10-dependent. Mech. Dev. 122, 659–669.

Frank, E., Sanes, J.R., 1991. Lineage of neurons and glia in chick dorsal root ganglia: analysis in vivo with a recombinant retrovirus. Development 111, 895–908.

Gammill, L.S., Bronner-Fraser, M., 2003. Neural crest specification: migrating into genomics. Nat. Rev., Neurosci. 4, 795–805.

Gilmour, D.T., Maischein, H.M., Nusslein-Volhard, C., 2002. Migration and function of a glial subtype in the vertebrate peripheral nervous system. Neuron 34, 577–588.

Greenwood, A.L., Turner, E.E., Anderson, D.J., 1999. Identification of dividing, determined sensory neuron precursors in the mammalian neural crest. Development 126, 3545–3559.

Gupta, P.B., Kuperwasser, C., Brunet, J.P., Ramaswamy, S., Kuo, W.L., Gray, J.W., Naber, S.P., Weinberg, R.A., 2005. The melanocyte differentiation program predisposes to metastasis after neoplastic transformation. Nat. Genet. 37, 1047–1054.

Hanna, L.A., Foreman, R.K., Tarasenko, I.A., Kessler, D.S., Labosky, P.A., 2002. Requirement for Foxd3 in maintaining pluripotent cells of the early mouse embryo. Genes Dev. 16, 2650–2661.

Hellqvist, M., Mahlapuu, M., Blixt, A., Enerback, S., Carlsson, P., 1998. The human forkhead protein FREAC-2 contains two functionally redundant activation domains and interacts with TBP and TFIIB. J. Biol. Chem. 273, 23335–23343.

Henion, P.D., Weston, J.A., 1997. Timing and pattern of cell fate restrictions in the neural crest lineage. Development 124, 4351–4359.

Hromas, R., Ye, H., Spinella, M., Dmitrovsky, E., Xu, D., Costa, R.H., 1999. Genesis, a Winged Helix transcriptional repressor, has embryonic expression limited to the neural crest, and stimulates proliferation in vitro in a neural development model. Cell Tissue Res. 297, 371–382.

Huang, X., Saint-Jeannet, J.P., 2004. Induction of the neural crest and the opportunities of life on the edge. Dev. Biol. 275, 1–11.

Inoue, A., Seidel, M.G., Wu, W., Kamizono, S., Ferrando, A.A., Bronson, R.T., Iwasaki, H., Akashi, K., Morimoto, A., Hitzler, J.K., Pestina, T.I., Jackson, C.W., Tanaka, R., Chong, M.J., McKinnon, P.J., Inukai, T., Grosveld, G.C., Look, A.T., 2002. Slug, a highly conserved zinc finger transcriptional repressor, protects hematopoietic progenitor cells from radiation-induced apoptosis in vivo. Cancer Cell 2, 279–288.

Kelsh, R.N., Eisen, J.S., 2000. The zebrafish colourless gene regulates development of non-ectomesenchymal neural crest derivatives. Development 127, 515–525.

Kelsh, R.N., Dutton, K., Medlin, J., Eisen, J.S., 2000. Expression of zebrafish fkd6 in neural crest-derived glia. Mech. Dev. 93, 161–164.

Kimmel, C.B., Miller, C.T., Kruze, G., Ullmann, B., BreMiller, R.A., Larison, K.D., Snyder, H.C., 1998. The shaping of pharyngeal cartilages during early development of the zebrafish. Dev. Biol. 203, 245–263.

Knecht, A.K., Bronner-Fraser, M., 2002. Induction of the neural crest: a multigene process. Nat. Rev., Genet. 3, 453–461.

Knight, R.D., Nair, S., Nelson, S.S., Afshar, A., Javidan, Y., Geisler, R., Rauch, G.J., Schilling, T.F., 2003. Lockjaw encodes a zebrafish tfap2a required for early neural crest development. Development 130, 5755–5768.

Kos, R., Reedy, M.V., Johnson, R.L., Erickson, C.A., 2001. The winged-helix transcription factor FoxD3 is important for establishing the neural crest lineage and repressing melanogenesis in avian embryos. Development 128, 1467–1479.

LaBonne, C., Bronner-Fraser, M., 2000. Snail-related transcriptional repressors are required in *Xenopus* for both the induction of the neural crest and its subsequent migration. Dev. Biol. 221, 195–205.

Labosky, P.A., Kaestner, K.H., 1998. The winged helix transcription factor Hfh2 is expressed in neural crest and spinal cord during mouse development. Mech. Dev. 76, 185.

LeDouarin, N., Kalcheim, C., 1999. The Neural Crest. Cambridge Univ. Press, New York.

Lister, J.A., Robertson, C.P., Lepage, T., Johnson, S.L., Raible, D.W., 1999. Nacre encodes a zebrafish microphthalmia-related protein that regulates neural-crest-derived pigment cell fate. Development 126, 3757–3767.

Luo, R., An, M., Arduini, B.L., Henion, P.D., 2001. Specific pan-neural crest expression of zebrafish Crestin throughout embryonic development. Dev. Dyn. 220, 169–174.

Luo, R., Gao, J., Wehrle-Haller, B., Henion, P.D., 2003a. Molecular identification of distinct neurogenic and melanogenic neural crest sublineages. Development 130, 321–330.

Luo, T., Lee, Y.H., Saint-Jeannet, J.P., Sargent, T.D., 2003b. Induction of neural crest in *Xenopus* by transcription factor AP2alpha. Proc. Natl. Acad. Sci. U. S. A. 100, 532–537.

Marcos-Gutierrez, C.V., Wilson, S.W., Holder, N., Pachnis, V., 1997. The zebrafish homologue of the ret receptor and its pattern of expression during embryogenesis. Oncogene 14, 879–889.

Moury, J.D., Jacobson, A.G., 1989. Neural fold formation at newly created boundaries between neural plate and epidermis in the axolotl. Dev. Biol. 133, 44–57.

Nakagawa, S., Takeichi, M., 1998. Neural crest emigration from the neural tube depends on regulated cadherin expression. Development 125, 2963–2971.

Odenthal, J., Nusslein-Volhard, C., 1998. Fork head domain genes in zebrafish. Dev. Genes Evol. 208, 245–258.

Pani, L., Overdier, D.G., Porcella, A., Qian, X., Lai, E., Costa, R.H., 1992. Hepatocyte nuclear factor 3 beta contains two transcriptional activation domains, one of which is novel and conserved with the *Drosophila* fork head protein. Mol. Cell. Biol. 12, 3723–3732.

Parichy, D.M., Mellgren, E.M., Rawls, J.F., Lopes, S.S., Kelsh, R.N., Johnson, S.L., 2000a. Mutational analysis of endothelin receptor b1 (rose) during neural crest and pigment pattern development in the zebrafish *Danio rerio*. Dev. Biol. 227, 294–306.

Parichy, D.M., Ransom, D.G., Paw, B., Zon, L.I., Johnson, S.L., 2000b. An orthologue of the kit-related gene fms is required for development of neural crest-derived xanthophores and a subpopulation of adult melanocytes in the zebrafish, *Danio rerio*. Development 127, 3031–3044.

Perez, S.E., Rebelo, S., Anderson, D.J., 1999. Early specification of sensory neuron fate revealed by expression and function of neurogenins in the chick embryo. Development 126, 1715–1728.

Pietri, T., Eder, O., Breau, M.A., Topilko, P., Blanche, M., Brakebusch, C., Fassler, R., Thiery, J.P., Dufour, S., 2004. Conditional beta1-integrin gene deletion in neural crest cells causes severe developmental alterations of the peripheral nervous system. Development 131, 3871–3883.

Pohl, B.S., Knochel, W., 2001. Overexpression of the transcriptional repressor FoxD3 prevents neural crest formation in *Xenopus* embryos. Mech. Dev. 103, 93–106.

Raible, D.W., Eisen, J.S., 1994. Restriction of neural crest cell fate in the trunk of the embryonic zebrafish. Development 120, 495–503.

Raible, D.W., Wood, A., Hodsdon, W., Henion, P.D., Weston, J.A., Eisen, J.S., 1992. Segregation and early dispersal of neural crest cells in the embryonic zebrafish. Dev. Dyn. 195, 29–42.

Reedy, M.V., Faraco, C.D., Erickson, C.A., 1998. The delayed entry of thoracic neural crest cells into the dorsolateral path is a consequence of the late emigration of melanogenic neural crest cells from the neural tube. Dev. Biol. 200, 234–246.

Rubinstein, A.L., Lee, D., Luo, R., Henion, P.D., Halpern, M.E., 2000. Genes dependent on zebrafish cyclops function identified by AFLP differential gene expression screen. Genesis 26, 86–97.

Sasai, N., Mizuseki, K., Sasai, Y., 2001. Requirement of FoxD3-class signaling for neural crest determination in *Xenopus*. Development 128, 2525–2536.

Schilling, T.F., Kimmel, C.B., 1994. Segment and cell type lineage restrictions during pharyngeal arch development in the zebrafish embryo. Development 120, 483–494.

Schilling, T.F., Kimmel, C.B., 1997. Musculoskeletal patterning in the pharyngeal segments of the zebrafish embryo. Development 124, 2945–2960.

Shepherd, I.T., Pietsch, J., Elworthy, S., Kelsh, R.N., Raible, D.W., 2004. Roles for GFRalpha1 receptors in zebrafish enteric nervous system development. Development 131, 241–249.

Stewart, R.A., Look, A.T., Kanki, J.P., Henion, P.D., 2004. Development of the peripheral sympathetic nervous system in zebrafish. Methods Cell Biol. 76, 237–260.

Thisse, C., Thisse, B., Schilling, T.F., Postlethwait, J.H., 1993. Structure of the zebrafish snail1 gene and its expression in wild-type, spadetail and no tail mutant embryos. Development 119, 1203–1215.

Thisse, C., Thisse, B., Postlethwait, J.H., 1995. Expression of snail2, a second member of the zebrafish snail family, in cephalic mesendoderm and presumptive neural crest of wild-type and spadetail mutant embryos. Dev. Biol. 172, 86–99.

Ungos, J.M., Karlstrom, R.O., Raible, D.W., 2003. Hedgehog signaling is directly required for the development of zebrafish dorsal root ganglia neurons. Development 130, 5351–5362.

Vogel, K.S., Weston, J.A., 1988. A subpopulation of cultured avian neural crest cells has transient neurogenic potential. Neuron 1, 569–577.

Weinberg, E.S., Allende, M.L., Kelly, C.S., Abdelhamid, A., Murakami, T., Andermann, P., Doerre, O.G., Grunwald, D.J., Riggleman, B., 1996. Developmental regulation of zebrafish MyoD in wild-type, no tail and spadetail embryos. Development 122, 271–280.

Westerfield, M., 1993. The Zebrafish Book. University of Oregon Press, Eugene, OR.

Whitlock, K.E., 2005. Origin and development of GnRH neurons. Trends Endocrinol. Metab. 16, 145–151.

Wilson, Y.M., Richards, K.L., Ford-Perriss, M.L., Panthier, J.J., Murphy, M., 2004. Neural crest cell lineage segregation in the mouse neural tube. Development 131, 6153.

Wu, W.S., Heinrichs, S., Xu, D., Garrison, S.P., Zambetti, G.P., Adams, J.M., Look, A.T., 2005. Slug Antagonizes p53-Mediated Apoptosis of Hematopoietic Progenitors by Repressing puma. Cell 123, 641–653.

Yan, Y.L., Hatta, K., Riggleman, B., Postlethwait, J.H., 1995. Expression of a type II collagen gene in the zebrafish embryonic axis. Dev. Dyn. 203, 363–376.

Yan, Y.L., Willoughby, J., Liu, D., Crump, J.G., Wilson, C., Miller, C.T., Singer, A., Kimmel, C., Westerfield, M., Postlethwait, J.H., 2005. A pair of Sox: distinct and overlapping functions of zebrafish sox9 co-orthologs in craniofacial and pectoral fin development. Development 132, 1069–1083.